Original Article
Cent Asian J Med Sci. 2022 Dec;8(4):212-222. https://doi.org/10.24079/CAJMS.2022.12.003

Central Asian Journal of Medical Sciences
CAJMS

Paranasal Sinuses Anatomic Variants and its Association with Chronic Rhinosinusitis in Mongolia

Altandush Enkhtaivan[1], Bayarmaa Enkhbat[2], Bayarmagnai Lkhagvasuren[3], Gan-Erdene Narantsolmon[1], Ganchimeg Palamdorj[1], Byambasuren Luvsandagva[1]

[1]Department of Otorhinolaryngology, School of Medicine, Mongolian National University of Medical Sciences, Ulaanbaatar, Mongolia; [2]Department of Pathology and Forensic Medicine, School of Biomedicine, Mongolian National University of Medical Sciences, Ulaanbaatar, Mongolia; [3]Department of Epidemiology and Biostatistics, School of Public Health, Mongolian National University of Medical Sciences, Ulaanbaatar, Mongolia

Submitted: November 28, 2022
Revised: December 5, 2022
Accepted: December 21, 2022

Corresponding Author
Altandush Enkhtaivan
Department of Otorhinolaryngology, School of Medicine, Mongolian National University of Medical Sciences, Ulaanbaatar 14210, Mongolia
Tel: + 976-9915-5171
E-mail: ealtandush@fchm.edu.mn

Objective: The aim of this study was to obtain the prevalence of nasosinus anatomic variations in a Mongolian population and to understand their importance and impact on the disease process, as well as their influence on surgical management and outcome. **Methods:** This study is a prospective review of retrospectively performed normal computed tomography (CT) scans of the nose and paranasal sinuses in the adult Mongolian population. **Results:** Of all CT scans that were reviewed, 53.7 % were of women patients and 46.3 % were of men patients. The mean age of the study sample was 45.6 ± 16.3 years. The most common anatomic variation after excluding Agger nasi cell was pneumatized crista galli, which was seen in 98.8 % of the scans. Anatomic variants with a potential impact on operative safety included Haller cell (13.3 %), concha bullosa (20.5 %), and paradoxical middle turbinate (27.3 %). In our study, we compared the measurements between the anterior ethmoid artery and adjacent anatomical structures in two groups. **Conclusions:** A wide range of regional differences in the prevalence of each anatomic variation exists. Understanding the preoperative CT scan is substantially important because it is the road map for the sinus surgeon. Detection of anatomic variations is vital for surgical planning and prevention of complications.

Keywords: Nasal Sinuses, Chronic Rhinosinusitis, Sinus Infections, Paranasal Sinuses, Anatomic Variants

Introduction

Computed tomography (CT) is more commonly used by otolaryngologists to analyze changes in the structure of the nasal and paranasal cavity, bone structure, mucosa, and ventilation than traditional imaging [1, 2]. Further, detection of anatomical structure and image differences in the nose and nasal cavity, as well as the detection of congenital anatomical changes using computed tomography using bone and soft tissue windows prior to rhinoplasty can help prevent surgical complications

due to anatomical features [3 - 5]. Researchers have found that the nose and nasal septum have many anatomical variations. The most common variants are Agger nasi cells, Haller's cell, sphenoethmoidal cell (Onodi's cell) and concha bullosa. On the other hand, less common variants included uncinate bulla, pneumatized crista galli as well as supraorbital cells. Also, it has been demonstrated that concah bullosa, Haller's cell, Onodi's cell, angular, paradoxical middle turbinate and hyperthrophy of the middle turbinate are the most important forms related to diagnosis and treatment [6, 7].

Most researchers believe that abnormalities of the anatomical structure of the nasal cavity contributes to chronic inflammation of the nasal cavity. In addition, preoperative evaluation based on a CT scan and a checklist will ensure the effectiveness and safety of maxillofacial surgery. Otolaryngologists use CT scans to determine the anatomical structure of the PNS and the associated complications, as well as to identify important structures and provide guidance during endoscopic surgery [8]. Scientists have identified the anatomical shapes of the nasal cavities of each nation. A study conducted by Mokhasanavisu et al to determine the frequency of anatomical variants, volumes of paranasal sinuses using computed tomography and to identify any difference between people of the Indian subcontinent and people from the north east Asian region revealed that there was no significant difference between the two groups. Moreover, on volumetric analysis sphenoid sinus volume was found to be higher in Indians without mongoloid features [9]. Another study of Gruszka et al showed that the most common anatomic variation was septum deviation followed by the Agger nasi cell and concha bullosa with a prevalence of 87.7 %, 83.2 %, and 54.8 % respectively in the Polish population. For the Turkish Cypriot population, the most common anatomic variation was Agger nasi cell followed by concha bullosa and supraorbital ethmoid cells with a prevalence of 81.6 %, 68 %, and 57.8 % respectively [10].

Accurate knowledge of the anatomical structure of nasal and cranial surgery, the predominant anatomical structure of the nasal cavity, and how it interacts with adjacent structures can help prevent patient from complications during and after rhinoplastic surgery [11, 12]. The basis of our study is the lack of research to determine certain forms of nasal anatomy in the Mongolian population and how these forms affect inflammation of the nasal cavity. Therefore, we have determined some variants and dimensions of the nasal anatomy of Mongolian healthy adults by CT analysis and compared healthy and pathological groups. We have aimed in this study was to obtain the prevalence of nasosinus anatomical variations in the Mongolian population and to understand their importance and impact on the disease process, as well as their influence on surgical management and outcome.

Material and Methods

Research design

We carried out a hospital based retrospective study. A total of 800 participants' hospital records, which were recorded between November 2019 and November 2020 in First Central Hospital of Mongolia (FCHM) were reviewed. The anatomical structure of the nasal cavity was determined by computed tomography of 400 relatively healthy patients, as a control group and 200 patients with CNS who served, as a case group by the ENT department of FCHM. The control group was matched with the case group by age.

Measurement classification

The uncinate processes were classified according to a method developed in 2001 by American scientists R. Landsberg and M. Friedman. If the uncinate is attached to the bone plate, it is classified as option 1, if it is attached to the middle turbinate, it is classified as option 2, if it is attached from the bone center, it is classified as option 3, and if it is attached from the base of the skull, it is classified as option 4.

The sphenoid sinus was classified by a method developed in 1961 by Swedish scientists G. Hammer, and S. Radberg. The lateral (sagittal) axis divides the sphenoid sinus into three categories. Conchal type: The degree of pneumatization is limited to the anterior portion of the sphenoid body and not reaching the level of the anterior wall of the sella turcica. Presellar type: Pneumatization extends up to the vertical level of the anterior wall of the sella turcica but not beyond that. Sellar type: Pneumatization extends beyond the level of the anterior wall of the sella turcica below the pituitary fossa and might reach posterior to the sella turcica "occasionally called postsellar type" Spjenoid sinus is divided into 3 categories by coronal plane. Previdian type: the Vidian canal and foramen rotundum are covered by 3mm of bone. Intercanal type:

Pneumatization reaches to middle of the foramen rotundum, the vidian canal is seen through the sphenoid sinus. Postrotundum type: Pneumatization continues beyond the foramen rotundum and the vidian canal and maxillary division of trigeminal nerve protrudes into sphenoid sinus.

The olfactory fossa was classified by a method developed in 1962 by the German scientist P. Keros. The depth of the olfactory fossa is < 4 mm for Keros 1, 4 - 7 mm for Keros 2, > 7 mm for Keros 3. The length was classified according to a method developed by Turkish scientist A. Enigun. The length of the olfactory cavity is 6 - 10 mm for Category 1, 11 - 15 mm for Category 2, and 16 - 20 mm for Category 3.

The size between the other anatomical structures of the ethmoidal anterior artery (EAA) is calculated as follows: Ethmoidal anterior and posterior artery space, orbital nerve space, space between ethmoidal posterior artery and skull base, space between EAA and lower wall of orbital wall. Space between EAA and nasal base, space between EAA and frontal wall of ethmoid bulla. space between EAA and frontal beak.

The deviation of the nasal septum was classified by a method developed in 1987 by the Croatian scientist R. Mladina.Type 1: unilateral vertical septal ridge in the valve region that does not reach the valve itself; Type 2: unilateral vertical septal ridge in the valve region touching the nasal valve; Type 3: unilateral vertical ridge located more deeply in the nasal cavity. Type 4: S-shaped; Type 5: Almost horizontal septal spur; Type 6: massive unilateral bone spur, and Type 7: variation of these types.

CT scan was performed with a Philips 128 coronary, axial, and frontal plane covering 3 mm per incision at a rotational speed of 0.35 seconds with 128 independent channels. The test results were processed in a RadiAnt DICOM Viewer 4.0.3.

Statistical analysis

We expressed continuous variables including body mass index, degree of axis correction, medial proximal tibial angle, and knee joint flexion and extension range as the mean and standard deviation and assessed normally distributed data using the Kolmogorov-Smirnov test. Categorical data such as sex, education level, and tobacco consumption were presented by frequencies and percentages. For categorical variables, a Chi-square test was carried out. The continuous variables between two groups were compared by the upaired t-test. The significance level set at $p < 0.017$ ($p = 0.05/3$). Statistical analysis was performed using STATA 13.0 software.

Ethical statement

The study was approved by the Research Ethics Committee of the Mongolian National University of Medical Sciences on June 21, 2019 (No. 2019/6-21). All patients signed an informed consent form before clinical examination and morphometric measurement.

Results

The survey included a total of 600 patients, 278 men (46.3 %) and 322 women (53.7 %). The average age of patients was 45.6 ± 16.3. Gender ratio was 1: 1.15 for male: female. We categorized the anatomical variants that may affect the paranasal sinus inflammation into the nasal cavity and the paranasal cavity, and identified some variants and dimensions using the CTG test. We determined anatomical variants included concha bulla, paradoxical turbinate, interlamellar cavity, uncinate, lower turbinate, and nasal septal deviation. Also the structure of the nasal cavity, which can contribute to chronic inflammation of the paranasal sinuses, including the concha bulla, paradoxical turbinate, interlamellar cavity, 4 types of uncinate attachment, and the lower turbinate was determined.

In our study, there were 32 (7.8 %) paradoxic and 22 (5.4 %) bullous in Group 1. In group 2, 41 (20.5 %) paradoxic and 55 (27.3 %) bullous turbinate ($p < 0.000$) were found to contribute to chronic inflammation of the nasal cavity. In group 1, the uncinate was attached to 228 (57.0 %) bone plates, and in group 2, 97 (48.5 %) were attached to the middle turbinate ($p < 0.000$). There was no statistically significant difference (Table 1). The deviation of the nasal septum was calculated using the internationally used Mladina classification (Table 2) which is divided into two main groups: so called 'vertical' deformities (types 1,2,3 and 4), and 'horizontal' ones (types 5 and 6) as well as the seventh type, named 'Passali deformity'.

The highest percentage was in group 1 with no nasal septum deviation (34.0 %), and in group 2 nasal septal deviation blocked osteameatal complex, type -3, 59 (29.5 %)). There are many varients of nasal anatomy. We studied nasal anatomical varients which can affect CRS included Haller's cell, Onodi's cell, frontal cell, olfactory fossa, and sphenoid sinus (Figure 2).

Table 3 shows anatomical variants of paranasal sinus.

Table 1. Some variants of nasal anatomy.

Anatomical variants	Case (n = 200)	Control (n = 400)	Total (n = 600)	p-value
Middle turbinate	**N (%)**	**N (%)**	**N (%)**	
Bullous	41 (20.5)	22 (5.5)	63 (26.0)	0.091
Paradoxical	55 (27.3)	32 (8.0)	87 (35.3)	
Interlamellar cavity	24 (12.0)	40 (9.9)	64 (21.9)	
Attachment of uncinate				
One	35 (17.5)	228 (57)	263 (74.5)	0.086
Two	97 (48.5)	144 (36.1)	241 (84.5)	
More than 3	68 (34.0)	27 (6.8)	95 (40.8)	
Hyperthropic lower turbinate				
Yes	104 (52.3)	201 (50.2)	305 (76.3)	0.065
No	96 (47.7)	199 (49.8)	295 (23.7)	

Table 2. Nasal septum deviation type.

	Case (n = 200)	Control (n = 400)	Total (n = 600)
Deviation types	**N (%)**	**N (%)**	**N (%)**
Type 1	21 (10.5)	59 (14.7)	80 (25.2)
Type 2	45 (22.5)	64 (16.0)	109 (38.5)
Type 3	59 (29.5)	26 (6.5)	85 (36.0)
Type 4	43 (21.5)	52 (13.0)	95 (34.5)
Type 5	19 (9.5)	46 (11,5)	65 (21.0)
Type 6	6 (3.0)	14 (3.5)	20 (6.5)
Type 7	1 (0.5)	3 (0.8)	4 (1.3)
No deviation	6 (3.0)	136 (34.0)	142 (37.0)

Table 3. Paranasal sinus anatomy varients.

Anatomy varients	Case (n = 200)	Control (n = 400)	Total (n = 600)	p-value
	N (%)	**N (%)**	**N (%)**	
Haller's cell				
Yes	56 (13.3)	9 (2.2)	65 (15.5)	0.001
No	144 (86.7)	391 (97.8)	535 (74.5)	
Onodi's cell				
Yes	61 (30.5)	30 (7.5)	91 (38.0)	0.001
No	139 (69.5)	370 (92.5)	509 (62.0)	
Agger nasi				
Yes	193 (96.5)	395 (98.8)	588 (99.5)	0.059
No	7 (3.5)	5 (1.2)	12 (0.5)	
Frontal cell				
Yes	84 (42.0)	222 (55.3)	306 (97.3)	0.010
No	116 (58)	178 (44.7)	294 (2.7)	
Supra bullar cell				
Yes	32 (16.3)	48 (12.1)	80 (28.4)	0.056
No	168 (73.7)	352 (87.9)	520 (71.6)	

Haller's cell was found in a group 1, 9 (2.2 %), in a group 2, 56 (13.3 %) ($p < 0.001$), Onodi's cell was found in a group 1, 30 (7.5 %), group 2, 61 (30.5 %) ($p < 0.001$). In group 2, 84 (42.0 %) agger nasi has been shown to affect chronic nasal inflammation ($p < 0.01$). The olfactory fossa is a very important anatomical structure located in the ethmoid bone in anterior part of the brain, containing the olfactory bulb and olfactory nerve. It is separated by a very thin bone, there is a high risk of injury during nasal laparoscopic surgery (Figure 3).

The depth of the olfactory fossa is classified by Keros (Table 4). In group 1, class 2, 91.8%, in group 2, classification 2, was found 63.5 % ($p < 0.001$). When the length was classified by the Yenigun method, Class 1 was 40.5 % in Group 1 and Class 1 was 38.5 % in Group 2 ($p > 0.05$). p. In the study of the anatomy of 184 patients with nasal congestion, the incidence was 41.8 % for Class 1, 53.3 % for Class 2, and 4.9 % for Class 3, which is close to our results. The sphenoid sinus is located in the central part of the base of the brain and borders on important anatomical structures such as the optic nerve, carotid artery, and vidian nerve. Researchers have reported that 0.4 - 0.5 % of optic nerve injuries and 0.1 - 0.3 % of carotid artery injuries occur during endoscopic surgery. Nowadays, with the rapid development of endoscopic surgery, techniques are being introduced for cranial surgery through the basal cavity.

In the lateral axis, the Sellar type in Group 1 was 278 (69.5 %) and the Sellar type in Group 2 was 95 (47.5 %). In the vertical axis, the Intercanal type was 235 (58.7 %) in Group 1 and the Intercanal type was 95 (47.5 %) in the group with CRS (Figure 4.5).

Researchers believe that the circumference of the sphenoid sinus and the distance of the frontal infundibulum are important in chronic inflammation of the nasal cavity. The anterior ethmoid artery is an essential structure to consider when performing endoscopic nasal surgery. 11.4 - 40 % of the population has an anomalous position of the ethmoidal anterior artery, while 0.6 - 1.6 % are prone to bleed during nasal endoscopic surgery.

In our study, we made some measurements between anatomical structures (Figure 6). PEA and AEA distance in group 1 is 16.1 ± 1.6 mm, in group 2 it is 15.8 ± 1.0 mm, PEA and optic nerve distance is 7.6 ± 0.9 mm in group 1, 6.9 ± 0.5 mm was found in group 2. By comparing the two groups, the size of the circumference of ethmoid bulla was statistically significant

Table 4. Olfactory fossa classification (Grade).

Olfactory fossa	Case (n = 200)	Control (n = 400)	Total (n = 600)	p-value
	N (%)	N (%)	N (%)	
Depth (grade)				
First	43 (21.5)	26 (6.0)	69 (11.5)	0.001
Second	127 (63.5)	367 (91.8)	494 (82.3)	
Third	30 (15.0)	7 (2.2)	37 (6.16)	
Length (grade)				
First	77 (38.5)	162 (40.5)	238 (39.7)	0.095
Second	110 (55.0)	220 (55.0)	330 (55.0)	
Third	13 (6.5)	18 (4.5)	31 (5.2)	

Table 5. Anatomical structure measurement (mm).

Variables	Case (n = 200)	Control (n = 400)	Total (n = 600)	p-value
	Mean ± SD	Mean ± SD	Mean ± SD	
Circumference of ethmoid bulla	30.0 ± 3.0	28.1 ± 2.9	29.05 ± 2.9	0.068
Frontal sinus infundibulum	6.9 ± 0.9	7.1 ± 1.3	7.0 ± 1.1	0.184
Anterior and posterior ethmoid artery	15.8 ± 1.00	16.1 ± 1.6	15.9 ± 1.3	0.091
PEA and optic nerve distance	6.9 ± 0.5	7.6 ± 0.9	7.2 ± 0.7	0.451

PEA – posterior ethmoidal arteries

(Table 5). In our study, we compared the meurements between anterior ethmoid artery and adjacent anatomical structures in two groups. AEA and skull base distance was 1.9 mm ± 0.2 (1.5 - 2.9 mm), AEA and Inferior orbital distance 20.3 mm ± 1.2 (17.5 - 24.5 mm), AEA and nasal floor distance was 48.5 mm ± 1.9 (46.5 - 52.0 mm) found in a group1. AEA and frontal wall of frontal beak distance was 17.8 mm ± 0.8 (15.2 - 19.4 mm), AEA and frontal beak distance was 15.4 mm ± 0.8 (13.2 - 17.7 mm found in a group 2. (Table6), (Figure 7).

Table 6. Measurement between AEA and anatomical other structure (mm).

Variables	Case (n = 200)	Control (n = 400)	Total (n = 600)	p-value
	Mean ± SD	Mean ± SD	Mean ± SD	
AEA and skull base distance	2.0 ± 0.2	1.9 ± 0.2	1.95 ± 0.20	0.095
AEA and inferior orbital distance	20.4 ± 1.1	20.3 ± 1.2	20.35 ± 1.15	0.125
AEA and nasal floor distance	48.5 ± 1.6	48.5 ± 1.9	48.5 ± 1.75	0.314
AEA and frontal wall of frontal beak distance	17.8 ± 0.8	17.1 ± 0.8	17.45 ± 0.80	0.719
AEA and frontal beak distance	15.4 ±0.8	15.3 ± 1.0	15.35 ± 0.9	0.682

AEA - anterior ethmoidal arteries

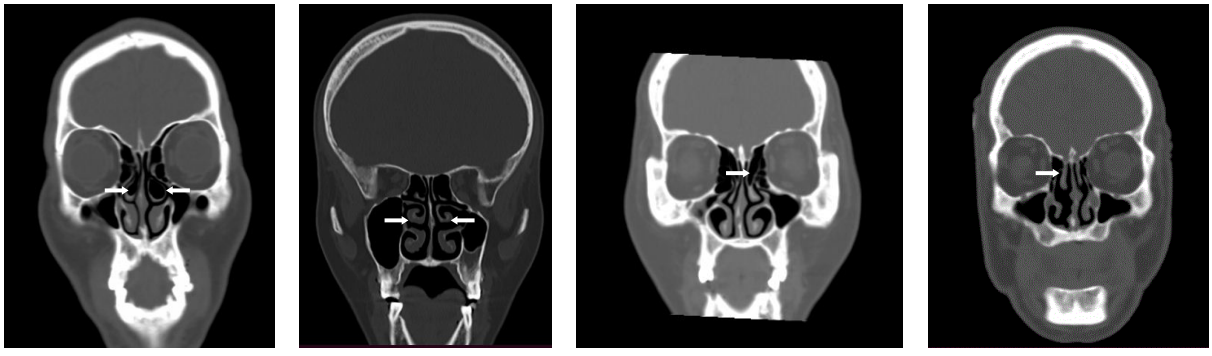

A B C D

Figure 1. Some variants of nasal anatomy (white arrow). A. Concha bulla. B. Paradoxical turbinate. C. Interlamellarcavity. D. Uncinate process (attached to middle turbinate)

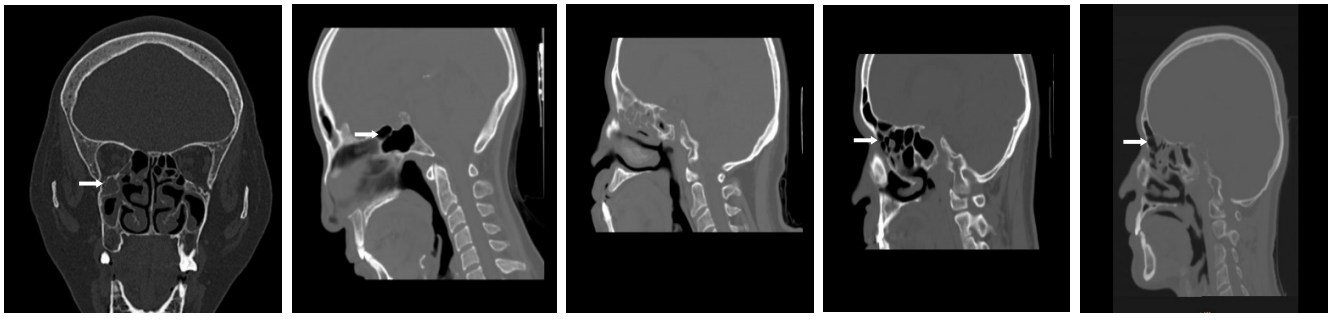

A B C D E

Figure 2. Some variants of nasal anatomy (white arrow). A. Haller's cell. B. Onodi's cell. C. Agger nasi. D. Frontal cell. E. Supra bullar cell

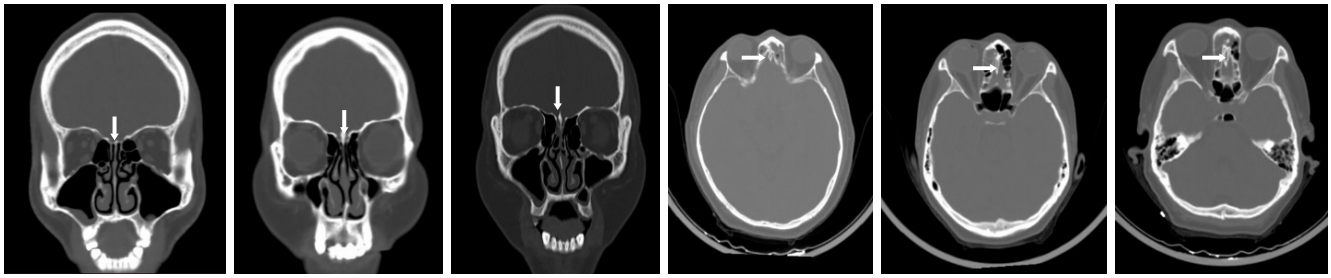

Figure 3. Olfactory fossa classification (white arrow). A. Keros -1. B. Keros -2. C. Keros -3. D. Yenigun -1. E. Yenigun-2. F. Yenigun -3.

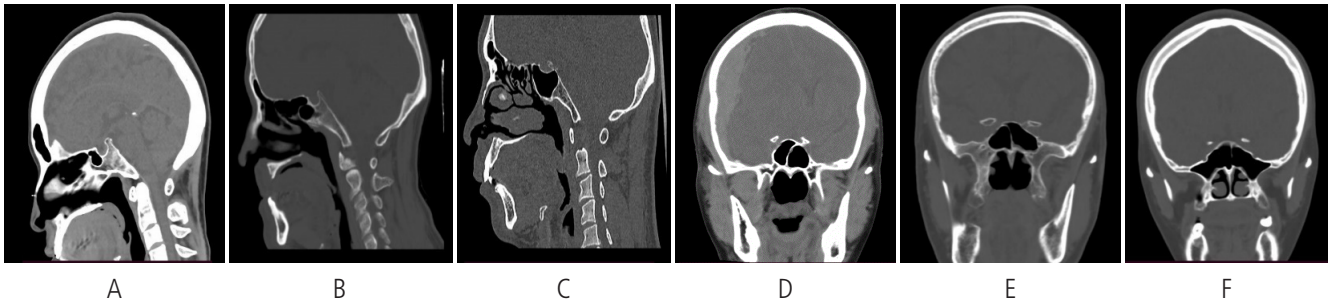

Figure 4. Variants of sphenoid sinus (saggital and coronal plane). A. Conchaltype. B. Presellartype. C. Sellartype. D. Previdian type. E. Intercanal type. F. Postrotundum type.

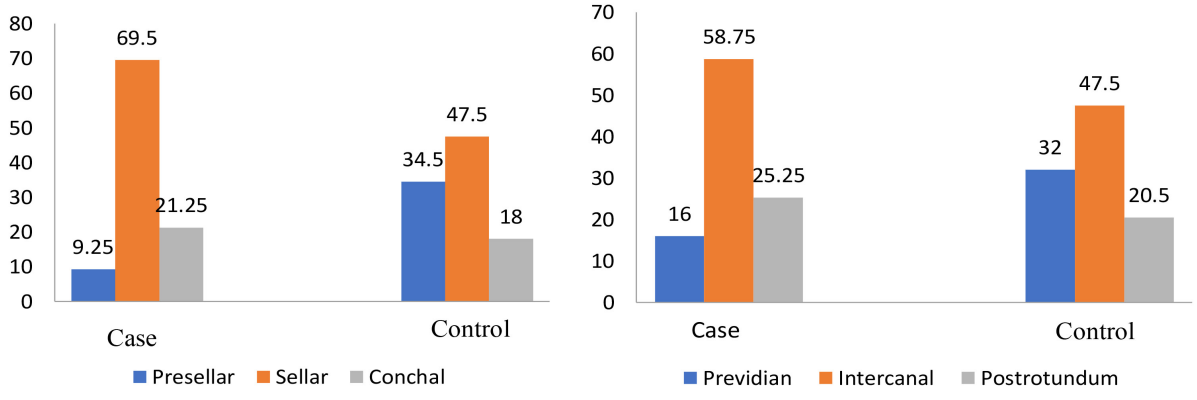

Figure 5. Sphenoid sinus variants (by percent)

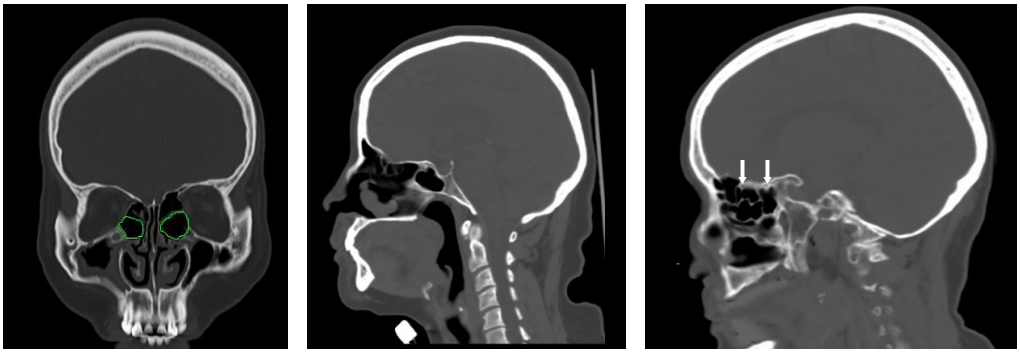

A B C

Figure 6. Some measurements made between anatomical structures. A. Circumference of ethmoid bulla (green round). B. Frontal infundibulum. C. Anterior and posterior ethmoid artery (white arrow).

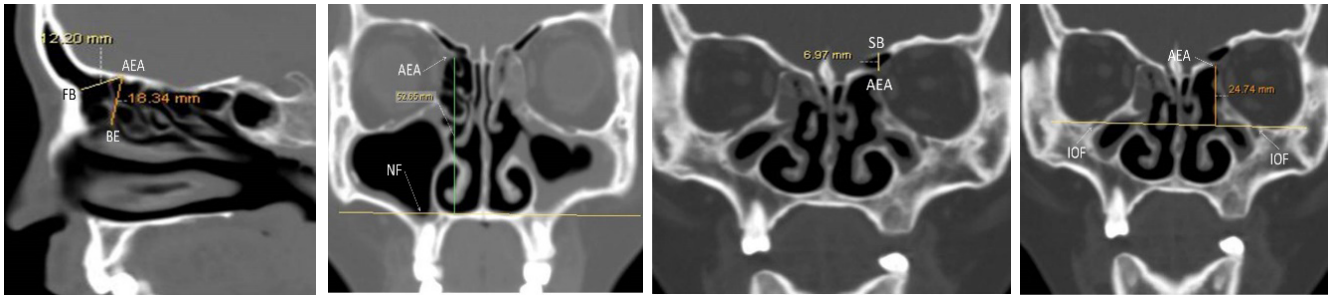

A B C D

Figure7. Measurement between AEA and anatomical other structures. A. Distance between AEA and skull base. SB-skull base, AEA - Anterior ethmoid artery. B. Distance between AEA and inferior orbital. IOF-Inferior orbital fissure. C. Distance between AEA and nasal floor. NF-Nasal floor. D. AEA and frontal beak, frontal beak space. FB -Frontal beak.

Discussion

Functional endoscopic sinus surgery is an advanced treatment that causes less tissue damage. For successful in surgery, it is important to know the anatomical structure of the nasal cavity. To do this, a CT scan should be performed on each patient prior to endoscopic surgery.

According to our study, the anatomical variant that affects the excretory function is the concha bullosa of the nasal cavity which differs by 5.4 % in the healthy group and 20.5 % in the group with CRS (17 % - 28 %) were noted. According to Adeel et al, it is 24 % - 55 % and according to Halil et al, it is 17 % - 28 % [13 - 14]. In our study of paradoxical middle turbinate, it was 7.8 % - 27.3 %. In the study of Kantarchi and others, 26 % of the 15 cases of paradoxical middle turbinate were reported [15].

Uncinate process is the anterior anatomical structure that occurs during sinus endoscopic surgery. According to Landsberg et al, the classification of attached part of the uncinate process has been revised. The researchers estimated that 52 % of uncinate process is attached to the lamina papyracea, 18.5 % to the agger nasi, 25.9 % to the middle turbinate, and 3.6 % to the skull base [16]. According to a study by Tuli, patients with CRS, in 63 % it was attached to the lamina papyracea and 16.7 % to the skull base [17]. According to Kumar and others, 19.0 % of uncinate process is attached to the lamina papyracea, 36.0 % to the agger nasi, 27.0 % to the middle turbinate and 8.0 % to the skull base [18]. From these, it can be seen that the attachment of anatomic variation of the uncinate process varies from nation to country.

The Haller cells consist of one, and sometimes several cells, usually located in the orbital inferior wall. In our study, the difference was 2.2 % in the Haller cells of the healthy group and 13.3 % in the CRS group. According to Grunwald, Van Alia,

Meloni, Zinrich, and Kennedy, Haller cells occurred at 4 %, 11 %, 10 %, and 10 %.

The olfactory fossa consists of the olfactory bulb and blood vessels. In 1962, Keros classified the olfactory fossa into three depths. W. Lund and H. Stamberger reported that Keros class 1 is 12 %, Keros class 2 is 70 %, Keros class 3 is 18 %, and asymmetrical structures on both sides are 10 - 30 %. In our study, Keros 1 class was 11.5 %, Keros 2 class was 82.3 %, and Keros 3 class was 6.3 %. which is approximately our result [19, 20]. The length of the olfactory cavity was classified into three groups according to a method developed by Turkish scientist A. Yenigun. We studies the anatomy of 184 patients with nasal and paranasal sinus disease. It has been reported that Category 1 was 41.8 %, Category 2 was 53.3 %, and Category 3 was 4.9 % [21].

In our study, the anatomical variant of the Onodi's cell was 15.2 %, which is located at the posterior to the ethmoid, anterior superior to the sphenoid. It occurs in 3.4 % - 14 % of the total population. The deviation of the nasal septum has a significant effect on respiratory function. Approximately 50 % of the deviation of the traumatic nasal septum is restored by nasal septal surgery. In 1954, the deviation of the nasal septum was classified as "C" and "S" curvature by Lindal [22]. Nowadays, there many other classifications are used. Deviation of the nasal septum is common in 81.7 % of the population, with the highest deviation occurring in the posterior inferior part at 16.6 % and in the inferior anterior at 11.7 % [23]. In our study, the deviation of the nasal septum was 76.4 % and the deviation of the inferior septum was 28.6 %. The curvature of the nasal septum occurs in 51.9 % of the Pakistani population according to Adiel and 67.3 % of the Spanish population according to Perez-Pinas, indicating that the anatomical shape of the nose and nasal cavity varies from nation to nation.The sphenoid cavity is an important anatomical structure bordering the optic nerve and the carotid artery. Sphenoid sinus is divided into 3 groups depending on pneumatization [24]. The cochal structure is located in anterior to the sphenoid bone, not bordering the anterior wall of the Turkish saddle, prevalence 1 % - 4 %. Ventilation of the presellar structure is 35 % - 40 % distributed, located adjacent to the anterior wall of the Turkish saddle. In terms of Sellar structure, the sphenoid ventilation is located posterior to the anterior wall of the Turkish saddle and reaches the pit of the pituitary gland, then goes to the posterior part of the Turkish saddle, and is distributed in 55 % - 60 % of the total population [25].

In our study, we made some measurements in addition to the anatomical shapes. The anterior and posterior arteries of the ethmoid arteries are branches of the orbital artery and supply blood to the nose, paranasal sinuses and nasal septum. In our study, distance between AEA and PEA was 15.9 ± 1.3 mm, distance between the PEA and optic nerve was 7.2 ± 0.7 mm. According to a study by Ashwini Mutalik, the distance between AEA and PEA was 13.9 ± 1.0 mm, and the distance between PEA and optic nerve was 6.4 ± 1.8 mm [26, 27].

Abdullah et al conducted a survey with 126 people from China, Malaysia and India and measured the AEA of 252 patients based on CT analysis. Classification of olfactory fossa by Keros was 41.4 % for type 1 and 58.6 % for type 2. Classified by Yenigun, 97.6 % for type 1 and 4 % for type 2. AEA and skull base distance was 1.93 ± 2.03 mm (0 - 7.50 mm), inferior orbital floor and AEA was 21.91 ± 2.47 mm (17.05 - 30.35 mm), AEA and nasal floor was 49.01 ± 3.53 mm (40.90 - 57.90 mm) [28].

In our study, anterior ethmoid artery and nasal floor was 48.5 ± 1.9 mm (46.5 - 52.0 mm). This was similar to the results of Moon's study of the Korean population (49.0 ± 4.9 mm), but was different from that of the European population of Arauho (61.72 ± 4.18 mm) and Monjas-Cánovas (55.51 ± 5.52 mm) [29 - 31]. The results of the study differ from those of the Asian population. In the study of Wuttiwongsanon CCP and others [32 - 34] among the Asian population, AEA and inferior orbital wall was 21.91 ± 2.47 mm, which is similar to our study. According to a study of 300 Brazilians by Bortoli et al, the distance between the anterior ethmoid artery and the anterior ethmoid bulla was 17.2 ± 1.8 mm. The distance to frontal beak was 15.1 ± 2.2 mm, which was similar to our study [35, 36].

Our study has some limitations. The variations of the anatomy of the nasal cavity depend on numerous factors such as age, race, geography and ethnicity. Therefore, study of sinonasal anatomic variants determined by multicenter options should be conducted further. Especially, without a longitudinal study design, the question remains as to what role climatic condition play in the sinonasal anatomy in the Mongolian population.

Conclusions

Inflammation of the nasal cavity is affected by some anatomical variants including nasal septum deviation, Haller's cell, ethmoid bulla, hypertrophied turbinate, and circumference of ethmoid

bulla in statistical significance. The study of the paranasal anatomical structure, especially the topography of the AEA, is important in choosing the method of endoscopic surgery and in preventing complications and risks that may occur during surgery depending on the anatomical shape.

References

1. Gupta A, Mahajan V, Gupta P, Jamwal P. Sinonasal anatomical variations in chronic rhinosinusitis. Kathmandu Univ Med J 2016; 14: 342-6.
2. Guler C, Uysal IO, Polat K, Salk I, Muderris T, Kosar MI, et al. Analysis of ethmoid roof and skull base with coronal section paranasal sinus computed tomography. Arch Craniofac Surg 2012; 23: 1460-4.
3. Nada AA. Anatomic variations of the nose and paranasal sinuses in saudi population: computed tomography scan analysis. Egypt J Otolaryngol 2018; 24: 234-41.
4. Aygun N, Zinreich SJ. Imaging for functional endoscopic sinus surgery. Otolaryngol Clin North Am 2006; 39: 403-16.
5. Midilli R, Aladag G, Erginoz E, Karci B, Savas R, et al. Anatomic variations of the paranasal sinuses detected by computed tomography and the relationship between variations and sex. Ear Nose Throat J 2005; 14: 49-56.
6. Jaworek JK, Troc P, Chrzan R, Sztuk S, Urbanik A, Walocha J, et al. Anatomic variations of the septation within the sphenoid sinus on CT scan images--an initial report. Przegl Lek 2010; 67: 279-83.
7. Bolger WE, Butzin CA, Parsons DS. Paranasal sinus bony anatomic variations and mucosal abnormalities: CT analysis for endoscopic sinus surgery. Laryngoscope 1991; 101: 56-64.
8. Zinreich SJ. Functional anatomy and computed tomography imaging of the paranasal sinuses. Am J M Sc 1998; 316: 2-12.
9. Prescher A. Clinical anatomy of the paranasal sinuses. Descriptive anatomy, topography and important variations. HNO 2009; 57: 1039-50.
10. Becker SS. Preoperative computed tomography evaluation in sinus surgery: a template-driven approach. Otolaryngol Clin North Am 2010; 43: 731-51.
11. Badia L, Lund VJ, Wei W, Ho WK. Ethnic variation in sinonasal anatomy on CT-scanning Rhinology 2005; 43: 210-4.
12. Adeel M, Rajput MS, Akhter S, Ikram M, Arain A, Khattak YJ, et al. Anatomical variations of nose and para-nasal sinuses; CT scan review. JPMA 2013; 63: 317-9.
13. Halil Alb, Mehmet B, Erol E. Anatomic variations of the paranasal sinuses: CT examination for endoscopic sinus surgery. Auris Nasus Larynx 1999; 26: 39-48.
14. Kantarci M, Karasen RM, Alper F, Onbas O, Okur A, Karaman A, et al. Remarkable anatomic variations in paranasal sinus region and their clinical importance. Eur J Radiol 2004; 50: 296-302.
15. Landsberg MMF. A Computer-assisted anatomical study of, the Nasofrontal region. Laryngoscope 2001; 111: 2125-30.
16. Isha P, Santosh PK, Suvamoy Ch. Anatomical variations of uncinate process observed. Indian J Otolaryngol Head Nech Surg 2013; 65: 157-161.
17. Kumar N, Kamala E, Vaithees G, Kumari S. A computerized tomographic study of uncinate process of ethmoid bone. IJAR 2015; 3: 917-21.
18. Keros P. On the practical value of differences in the level of the lamina cribrosa of the ethmoid. Z Laryngol Rhinol Otol 1962; 41: 809-13.
19. Lund V, Stammberger H, Fokkens W. European position paper on the anatomical terminology of the internal nose and paranasal sinuses. Rhinology 2014; 50: 1-34.
20. Alper SSG, Remzi D, Sabri BE, Orhan O. A study of the anterior ethmoidal artery and a new classification of the ethmoid roof (Yenigun classification). Eur Arch Otorhinolaryngol 2016; 19: 201-11.
21. Weinberger DG, Anand VK, Al-Rawi M, Cheng HJ, Messina AV, et al. Surgical anatomy and variations of the onodi cell. Am J Rhino 1996; 6: 365-70.
22. Teixeira J, Certal V, Chang ET, Camacho M. Nasal septal deviations: a systematic review of classification systems. Plast Surg Int 2016; 2: 708-91.
23. Madani SA, Hashemi SA, Modanluo M. The incidence of nasal septal deviation and its relation with chronic rhinosinusitis in patients undergoing functional endoscopic sinus surgery. JPMA 2015; 65: 612-4.
24. Güldner C, Pistorius SM, Diogo I, Bien S, Sesterhenn A, Werner JA, et al. Analysis of pneumatization and neurovascular structures of the sphenoid sinus using cone-beam tomography (CBT). Acta radiol 2012; 53: 214-9.
25. Mutalik A, Kolagi S, Hanji C, Ugale M, Rairam GB. A

morphometric anatomical study of the ethmoidal foramina on dry human skulls. JCDR 2011; 5: 28-30.
26. Baharudin EHL, Hazama M, Salina H, Mohd EA, Kornkiat S, Wang DY, et al. Anatomical variations of anterior ethmoidal artery at the ethmoidal roof and anterior skull base in Asians. Surg Radiol Anat 2019; 41: 543-50.
27. Moon HJ, Lee JG, Chung IH, Yoon JH. Surgical anatomy of the anterior ethmoidal canal in ethmoid roof. Laryngoscope 2011; 111: 900-4.
28. Araujo WR, Pinheiro CD, Lessa MM, Voegels RL, Butugan O, et al. Endoscopic anatomy of the ante rior ethmoidal artery: a cadaveric dissection study. Rev Bras Otor rinolaringol 2006; 72: 303-8.
29. Monjas-Cánovas IG-GE, Arenas-Jiménez JJ, Abarca-Olivas J, Sánchez-Del Campo F, Gras-Albert JR, et al. Radiological anatomy of the ethmoidal arteries: CT cadaver study. Acta Otorrinolaringol Esp 2011; 62: 367-74.
30. Wuttiwongsanon CP, Harvey RJ, Sacks R, Schlosser RJ, Chusakul S, Aeumjaturapat S, et al. The orbital floor is a surgical landmark for the Asian anterior skull base. Am J Rhinol Allergy 2015; 29: 216-9.
31. Vinicius RFM, Krystal CN. Study of anthropometric measurements of the Anterior ethmoidal artery using threedimensional Scanning on 300 Patients. IAO 2017; 21: 15-20.
32. Bortoli VT, Martins RF, Negri KC. Study of Anthropometric Measurements of the Anterior Ethmoidal Artery using Three-dimensional Scanning on 300 Patients. Int Arch Otorhinolaryngol 2017; 21: 115-21.
33. Sivasli E, Sirikçi A, Bayazýt YA, Gümüsburun E, Erbagci H, Bayram M, et al. Anatomic variations of the paranasal sinus area in pediatric patients with chronic sinusitis. Surg Radiol Anat 2003; 24: 400-5.
34. Nouraei SA, Elisay AR, Dimarco A, Abdi R, Majidi H, Madani SA, et al. Variations in paranasal sinus anatomy: implications for the pathophysiology of chronic rhinosinusitis and safety of endoscopic sinus surgery. J Otolaryngol Head Neck Surg 2009; 38: 32-7.
35. Shpilberg KA, Daniel SC, Doshi AH, Lawson W, Som PM, et al. CT of anatomic variants of the paranasal sinuses and nasal cavity: poor correlation with radiologically significant rhinosinusitis but importance in surgical planning. Am J Roentgeno. 2015; 204: 1255-60.
36. Gruszka K, Aksoy S, Różyło-Kalinowska I, Gülbeş MM, Kalinowski P, Orhan K, et al. A comparative study of paranasal sinus and nasal cavity anatomic variations between the Polish and Turkish Cypriot Population with CBCT. Head Face Med 2022; 26; 18: 37-41.